NASA Technical Memorandum 103935

P.19

A CFD Validation Roadmap For Hypersonic Flows

Joseph G. Marvin

April 1992

Presentation Paper - This report was presented at the 70th Fluid Dynamics Panel Meeting and Symposium on Theoretical and Experimental Methods in Hypersonic Flows, Torino, Italy, May 4-8, 1992.

National Aeronautics and Space Administration

NASA Technical Memorandum 103935

A CFD Validation Roadmap For Hypersonic Flows

Joseph G. Marvin, Ames Research Center, Moffett Field, California

April 1992

National Aeronautics and
Space Administration

Ames Research Center
Moffett Field, California 94035-1000

A CFD Validation Roadmap For Hypersonic Flows

Joseph G. Marvin
NASA Ames Research Center
MS 229-1
Moffett Field, CA 94035-1000
U. S. A.

1. SUMMARY
A roadmap for CFD code validation is developed. The elements of the roadmap are consistent with air-breathing vehicle design requirements and related to the important flow path components: forebody, inlet, combustor, and nozzle. Building block and benchmark validation experiments are identified along with their test conditions and measurements. Based on an evaluation criteria, recommendations for an initial CFD validation data base are given and gaps identified where future experiments would provide the needed validation data.

2. INTRODUCTION
Computational Fluid Dynamics (CFD) must play a major role in the development of aerospace vehicles because ground test facilities are not able to fully simulate flight conditions. A CFD code's accuracy must be determined by a validation process, however, because of possible sources of error in the solutions. The process of validation involves two aspects: numerical and experimental. Numerical validation is necessary because CFD codes provide approximate solutions to the governing equations; they use discrete grids; they employ algorithms that contain numerical dissipation; and they may have nonconvergence errors. Validation of a code's physical modeling and its application to complex flows requires experiment to determine accuracy limits and range of applicability. Consequently, the pace of CFD's introduction and the extent of its reliability depends on validation.[1]

The second aspect of validation depends on comparisons with well-posed experiments. Since code applications are becoming more complex, it no longer suffices to use data from surface or integral quantities such as lift and drag to provide the validation. Two types of experiments are essential to the determination of CFD accuracy.[2] Building block experiments are necessary to validate physical and chemical modeling. Special attention must be given to measurements necessary to guide and validate the modeling. Benchmark experiments are necessary to validate CFD code prediction capabilities. Measurements illuminating the ability to predict engineering quantities are required.

Shortcomings in CFD validation exist at all flight regimes, but especially at hypersonic speeds. Gaps exist in the validation data base at true flight enthalpy due to facility and instrumentation limits. Nevertheless, there is a need to review the current data base to determine whether or not it can provide a basis for initiating a CFD validation process. Furthermore, much can be gained by assembling the data base and making CFD comparisons so that the inevitable pitfalls can be avoided in planning new validation activities.

The purpose of this paper is to propose a validation roadmap consisting of a series of steps that can establish a code's capabilities and associated accuracy. A series of appropriate experiments will be identified and cataloged. Selected validation experiments will be identified and cataloged according to the flow path for an air-breathing vehicle, e.g., forebody, inlet, combustor, and nozzle. Some examples taken from the data base will be used to clarify and demonstrate their utility and applicability.

3. VALIDATION ROADMAP
For the purposes of this paper, validation will be used to imply an established correspondence between actual flows and those produced by computation. The author, together with colleagues from various NASA Research Centers, developed the following five-step validation roadmap: (1) Define what critical performance information is needed and establish the corresponding code requirements; (2) Establish the appropriate governing equations and the corresponding physical and/or chemistry modeling requirements; (3) Identify or develop the appropriate validation data (building block data to guide and validate modeling and benchmark data to validate complex flow computations); (4) Perform computations for exact experimental conditions and test their sensitivity to the numerical and modeling assumptions; and (5) Document the code including its validation to the extent necessary to provide users with knowledge of the code's sensitivity to internal numerical parameters, grid refinement effects, the code's accuracy, and range of capabilities.

4. REQUIREMENTS
CFD performance estimates to support the design of an air-breathing vehicle can be accomplished with "nose to tail" computations using a series of codes identified with the air flow path, i.e., forebody, inlet, combustor, and nozzle codes. Following the first two steps in the roadmap, vehicle component performance, code, and modeling requirements are introduced.

4.1 Forebody
The design performance requirements are lift, drag, and heat load. To predict these, a code is required to compute surface pressures, skin friction, heat transfer rates, and provide inlet flow profile conditions required to initiate the inlet component code. Modeling requirements are subdivided into numerical and physical categories. Numerically, it is essential to preserve mass, momentum, and energy, to capture discontinuities such as shock waves, and to compute or admit flows developed by blunt noses or leading edges to capture any entropy layer development. Code sensitivity to grid refinement, numerical dissipation, lack of convergence, and any internal code parameters must be determined and specified. Physical and chemistry modeling is required for transition, turbulence, shock interactions, entropy layer swallowing, equilibrium, nonequilibrium air chemistry, wall catholicity, and low density flow at high altitudes. Mach number, Reynolds number, and forebody structural material will determine the modeling needs for air chemistry.

4.2 Inlet

The design performance requirements are mass capture, kinetic energy efficiency, pressure recovery, heat load, and spillage drag. To predict these the code is required to compute wall pressures, skin friction, heat transfer, mass flow, and provide exit profiles for the initial conditions of the combustor component code. Numerical, physical, and chemical modeling requirements are similar to those described previously for the forebody, but the code must additionally model cowl shock interactions and separation resulting from shock/boundary-layer interaction.

4.3 Combustor

Thrust, heat load, efficiency, pressure losses, and structural loads are the performance requirements of concern in the design. Codes are required to compute overall thrust, wall pressures, skin friction, heat transfer, and provide the flow exit profiles needed to initiate the nozzle component codes. Complex situations involving vortex and injector interactions with the main flow must be modeled in these codes. Numerical and mathematical modeling requirements are essentially the same as those listed previously, but it is essential that these codes handle finite rate chemistry, including air-fuel reactions, and that they model turbulence chemistry interactions.

4.4 Nozzle

Thrust, moments, and heat loads are the performance parameters required for design. The codes are required to predict net thrust, wall pressures, heat transfer, and skin friction. Physical and chemical modeling requirements include turbulence, shock interactions, shear layers, relaminarization, secondary flows, and finite rate chemistry for the air-fuel products of combustion.

5. VALIDATION DATA BASE

The next roadmap step is to identify or develop an appropriate data base. Candidate experiments for CFD validation were identified through literature searches and knowledge of recent validation activities within the U.S.A. They were divided into the building block and benchmark categories referred to previously and integrated into a matrix table. The tables were then used to show the range and completeness of the data, to identify gaps, and to select an initial validation data base.

A portion of the results are shown in tables 1–7 for each component category. The experiments, listed across the top of the table in numerical sequence according to reference number, were checked against the physical and chemical modeling requirements and performance requirements for the building block and benchmark experiments, respectively. (There is no significance attached to the numbering order.) Brief notations of test conditions and geometry are given. Measurements from the experiments were then checked to determine their match with the requirements.

Several important conclusions can be drawn from a study of the tabular results. The number of benchmark experiments is substantially fewer than the number of building block experiments, partly because component testing is often proprietary and not generally accessible. While the range of Mach numbers extends into the hypersonic regime, the enthalpy at which the experiments were conducted is mostly not commensurate with flight enthalpy and hence few "real gas" sets of data are available. The number of combustor and nozzle experiments lags considerably compared to the other categories and no combustor benchmark data are available to the general user. The types and variety of measurements for any single experiment and from experiment to experiment varies considerably, reflecting the fact that experiments performed in former decades were not planned to satisfy the needs of validation and that instrumentation and facilities, even today, limit our ability to perform complete validation experiments. Nevertheless, selected experiments from this data base provide the basis for initiating a focused validation effort.

5.1 Selection Criteria

The criteria for selecting the building block experiments were as follows: The data were required to be performed at conditions matching hypersonic flight Mach numbers ($M > 3$) for single flows associated with components of an air-breathing vehicle; they had to provide enough useful data to test specific physical or chemical modeling problems; they had to have boundary conditions defined sufficiently to initiate CFD solutions; and they had to have experimental errors identified and their specificity was desired. To the extent possible with today's status of instrumentation and facility development, measurements of flow field quantities and at least some measurement redundancy was desirable.

The selection of the benchmark experiments was made using a similar basis. Measurement details on flow modeling and chemistry, desirable for the building block data base, were not considered essential so long as the data reflected a measure of the actual physics and chemistry. However, test cases were sought that could test a code's ability to predict performance over a range of flow conditions. To the extent possible, measurements of flow field quantities in critical regions of the flow were desirable.

6. RECOMMENDED EXPERIMENTS

These are sketched in figs. 1–7 and listed by reference number. Although the experimental data base has shortcomings and gaps, it is assumed that code developers can use it collectively to provide a much needed validation baseline. Adhering to it can establish the physical and chemical modeling attributes of the codes, establish credibility regarding performance prediction, and establish important code-to-code comparisons for added confidence. Furthermore, code developers and experimentalists can use the information as a guide to improving and enhancing current experiments or for proposing additional ones.

6.1 Forebody

Transition, turbulence, and air chemistry are the most critical modeling issues. Selected building block experiments are given in fig. 1.

Transition onset and extent, influence of pressure gradient and bluntness, and influence of three-dimensional flow all must be modeled. At present, transition modeling is ad hoc and founded on experimental evidence influenced by uncertainties associated with free stream flight or wind tunnel conditions. Nevertheless, some experiments were selected in order to assess and compare current transition modeling. Experiment 1 is a flight experiment useful in assessing transition onset criteria for high Mach number real gas conditions. The remaining group of wind tunnel experiments are recommended for assessing the ability to model trends with bluntness and the influence of 3-D effects with the

understanding that wind tunnel disturbances influence the actual locations of transition, if not the trends. NASA Langley Research Center's development of disturbance-free, quiet wind tunnels will provide much better validation data in the future. Experiment 3 was one of the first quiet wind tunnel demonstration experiments.

The validation experiments for attached flows selected for assessing turbulence modeling cover a range of Mach numbers, are limited in wall cooling range to 0.2, and the majority do not simulate flight enthalpies. (The latter may not present a major impediment as the influence of turbulence-chemistry interaction is not believed to be a first-order effect, except in combustor and nozzle flows.) Validation studies to date show turbulence modeling for attached hypersonic flows is reasonably in hand (see, e.g., ref. 60). Uncertainties remain in modeling the influence of pressure gradients, however, and a data base is only available at lower Mach numbers. One experiment on a conical configuration is available for assessing modeling for forebodies at angle of attack.

Air chemistry modeling is essential to numerical computations of hypersonic flows. Implementation of equilibrium air chemistry in CFD codes is straightforward and has a sound basis. Nonequilibrium air chemistry implementation in CFD codes is less advanced, e.g., decisions regarding strong or weak coupling of the species equations with the fluid dynamics equations and the choice of rate constants. Therefore, the recommended experiments involve conditions where nonequilibrium chemistry modeling is needed. The sharp and blunt cone data from a ballistic range test for laminar flow conditions in air provides a unique set of experiments conducted for this purpose. Other experiments in heated oxygen and nitrogen are also available. The paucity of detailed experimental profile data apropos to validation at flight enthalpies for both equilibrium and nonequilibrium flows suggests that code-to-code comparisons become an integral part of the validation process. With this objective in mind it is also recommended that code-to-code comparisons be made for the altitude and velocity conditions specified in cases 1 and 2 of ref. 61 for testing nonequilibrium modeling and case 2-b from ref. 62 for testing equilibrium modeling.

The recommended benchmark experiments are given in fig. 2. Only two experiments are recommended and they provide data on generic geometries at hypersonic Mach number and Reynolds number conditions leading to both laminar and turbulent flow. (The data from experiment no. 46 are currently restricted to U.S. citizens with access to NASP information.) The test conditions do not match flight enthalpies and corresponding air chemistry reactions. These experiments, however, will serve to validate 3-D algorithms, incorporation of transition and turbulence models in them, and performance predictions of aerodynamic parameters.

6.2 Inlet

Transition, turbulence, and air chemistry are also important modeling issues associated with developing inlet codes. In addition however, shock-wave/boundary-layer interaction modeling is crucial. The building block experiments selected for the validation data base are listed in fig. 3.

In addition to those previously selected and discussed for transition, turbulence, and chemistry modeling for the forebody, the remainder deal with the shock-wave/boundary-layer interaction problem for laminar and turbulent flows. A comprehensive search for turbulent shock interaction validation experiments was conducted for NASA by Settles.[63] Most of those experiments were listed in the candidate data base shown previously and a few are recommended herein. Additionally, recent turbulent validation experiments performed at NASA Ames Research Center have been selected. They provide data on flows with compression ramps, impinging shocks, and swept and intersecting shocks. All of the selected experiments were performed in wind tunnels at enthalpies that do not match flight.

Inlet benchmark experiments selected for the validation data base are shown in fig. 4. The Mach number range is limited and flight enthalpy is not matched. Although more experiments have been performed recently, they could not be recommended because they were performed on proprietary geometries. Nevertheless, the experiments selected will serve to validate 3-D algorithms, incorporation of turbulence modeling, and provide some data to evaluate predictions of performance parameters.

6.3 Combustor

The critical modeling issues for supersonic combustors involve various mixing processes of chemically reacting constituents. The combustor building block experiments shown in fig. 5 can be useful in assessing modeling of various mixing processes with and without chemical reactions, although they are limited in many instances by the variety and accuracy of their data.

Experiment 34 provides supersonic data for 3 nonreacting ejector flows: jet-off, jet-on , and two streamwise-aligned jets-on. Experiment 37 provides subsonic data for a reacting flow case. Experiment 36 and the data correlation from ref. 39 provide data to assess turbulence modeling of single and two-stream shear layers, and experiments 35, 38, and 40 provide shear layer mixing data for hydrogen-air reacting flows.

No combustor component experiments were selected because of their proprietary nature. There is still, nevertheless, a serious gap in both the combustor building block and benchmark experimental data base adequate for CFD validation.

6.4 Nozzle

The nozzle building block experiments selected for assessing modeling issues are shown in fig. 6. Of the critical modeling issues, turbulent boundary layer development and the expansion of reacting hydrogen-air mixtures are addressed.

Some of the flat plate flows from the forebody recommendations can be used to test implementation of turbulence models into nozzle codes. In addition, experiment 41 provides data on a turbulent boundary layer developing on a nozzle wall to a very high Mach number in helium. The data can be used to assess turbulence modeling for highly expanding nozzle flows. Experiments in nozzles with reacting air chemistry are lacking. Therefore a numerical test case developed recently and described in ref. 45 is recommended for code-to-code comparisons.

Only one nozzle benchmark experiment is recommended (see fig. 7). This particular experiment was designed with CFD Navier-Stokes codes under development at NASA Ames Research Center and was recently completed. Although it is a cold-air nozzle experiment, it can provide a basis for validation of 3-D algorithms, turbulence modeling, and the ability of the codes to predict some of the required performance parameters. Experiments with reacting air chemistry are needed.

7. RECENT VALIDATION ACTIVITIES

Some of the selected validation experiments were designed and carried out recently at the NASA Ames Research Center. Building block experiments at hypersonic Mach numbers were performed to guide and validate turbulence and real gas air chemistry modeling. Benchmark experiments were performed to validate 3-D forebody and nozzle codes. Each of the experiments was designed with validation as their primary purpose and some of the results are described next.

7.1 Physical and Chemical Modeling Experiments

Experiments designed to provide guidance and validation for the development of compressible turbulence models for various shock-wave/boundary-layer interactions have been accomplished in the Ames 3.5-Foot Hypersonic Wind Tunnel (3.5' HWT). Four experiments[21,30,33] were completed, providing surface measurements and mean-flow boundary layer profiles. Turbulence measurements will be obtained in the future with a laser anemometer and a laser-induced-fluorescence instrument developed for the facility.

One of these experiments consisted of a series of axisymmetric flares preceded by a cone-ogive-cylinder. The test geometry and conditions are shown in fig. 8. Beginning and end of transition occurred on the cone ahead of the cylinder. The measurements in the interaction zones included surface pressure, heat transfer, and surface oil streaks. A few mean flow velocity and density profiles were also obtained ahead of the interaction zone and on the 20° flare. The data are summarized and tabulated in ref. 21.

Experimental surface pressure and heat transfer distributions are shown in fig. 9 for the 35° flare. The separation locations determined from surface oil streaks are shown along with typical data error bars. The data are being used to validate turbulence model corrections for compressibility. They are compared with computations by Horstman[64] using a standard k-e eddy viscosity model and one corrected for compressibility. These solutions were obtained by solving the Reynolds-averaged Navier-Stokes equations. ITW refers to "integration to the wall" using low Reynolds number damping terms. For the modified model, which accounts for compressibility effects and limits the length scale in the vicinity of reattachment, significant improvements were obtained in predicting the measured pressure distribution, the predicted separation location, and the heat transfer.

Other tests were performed to guide turbulence modeling for impinging, swept, and intersecting swept shocks interacting with a turbulent boundary layer. A model sketch is shown in fig. 10. A sharp flat plate was used for these experiments. The plate was pitched at –2° angle of attack to increase the test Reynolds number and provide a uniform 2-D flow field on the plate. The plate was of a hollow frame construction, having interchangeable panels with several 20-cm-diameter holes in the center that accommodated surface pressure, heat transfer, pitot-static, yaw, and total temperature instrumentation ports. Tests were made with a wedge mounted above the test bed to generate a shock wave which impinged on the test bed. Pressure and heat transfer were measured throughout the interactions. In addition, to surface pressures and heat transfer, flow field surveys and skin friction were measured. Wedges with angles of 5°, 10°, and 15° were tested. In another configuration, fins were placed on the flat plate to generate a glancing shock-wave interaction. Fin angles of 5° to 15° were investigated. More recently a crossing shock interaction experiment was completed. In addition to surface pressure and heat transfer, flow field surveys and skin friction were obtained. Documented data are provided for each of these experiments.[30,33]

Typical data from the swept shock experiment are shown in fig. 11. Measured pressure and heat transfer, normalized by the upstream flat plate values, are plotted as a function of spanwise distances. Error bars are shown at two locations to indicate the variations in accuracy of the measurements. As the fin angle is increased, the corresponding increase in its shock strength causes the flow to separate, as observed from converging surface streamline patterns. Corresponding increases in heating and pressure were observed between 5 and 10 cm. As the fin wall is approached the pressures and heating continue to increase. On the fin the flow is laminar above the interaction and near the plate surface. Fin pressures (not shown) decrease rapidly at the intersection with the plate indicating the presences of a corner vortex.

Comparisons of the data on the plate with the 10° fin are compared with computations by Horstman[65] in fig. 12. Pressure, heat transfer, and skin friction data predicted with the Navier-Stokes code computations using a k-e model are in good agreement with the data. Although not shown here, comparisons of predictions with flow field profile data were also in good agreement. Evidently, for these flows, compressibility corrections needed for the strong 2-D interactions where large streamwise separations occurs are not required. Modeling studies on this flow are continuing, however.

Another building block experiment[10] has been carried out to obtain aerodynamic data at true flight enthalpy on sharp and blunt slender cones to assist in validating air chemistry modeling. It was carried out in the Ames Hypervelocity Ballistic Range at speeds in excess of 5 km/s. Reynolds numbers were between 10^5 and 10^6 and the flow was laminar. The resulting set of data is suitable for testing air chemistry modeling. Aerodynamic data for a 30% blunt 5° cone with conical ring shock generators were obtained and a summary of the important results taken from ref. 11 are shown in fig. 13. Aerodynamic data and a typical shadowgraph are shown and compared with computations by Molvik using a Navier-Stokes code with a strongly coupled 7-species air chemistry model and an ideal gas model. A histogram is shown for the number of data points used to deduce the aerodynamic coefficients. Confidence in the reported coefficients is greatest at moderate angles, where the number of data points is greatest. The top data figure shows the experimental and computed drag coefficient. The computed values of C_D using both perfect gas and real-gas chemistry models lie within the experimental error bars as one would expect, since the drag is mostly associated with the blunt nose. On the other hand, the

pitching moment is quite sensitive to the gas modeling because the cone surface pressures resulting from the gas expansion are affected by gas composition. The reacting gas model calculations provide a good prediction of the results. The shadowgraph is compared with pressure contours, and the shocks from the ring generators, which are also sensitive to gas composition, compare nicely.

A finite fringe interferogram was obtained during one range firing of a smooth blunted cone to provide validation information on flow field density.[66] However, obtaining density was more difficult than first anticipated because of pitch and yaw orientations of the model, the test density level, and because of the index of refraction's implicit dependence on density. Rather, it is now proposed that optical path be computed from the computations using real gas modeling and subsequently compared with the measured optical path. In fig. 14 the infinite fringe interferogram and interpreted optical path through the model wake are shown. As can be seen, the optical path data may provide an alternative, more sensitive means of validating the computations.

7.2 Generic All-Body Hypersonic Benchmark Experiment

A model of a generic hypersonic vehicle was tested in the NASA Ames 3.5-Foot Hypersonic Wind Tunnel to establish a benchmark experimental data base for validation of forebody computer codes. Experimental data on flow visualization, surface pressures, surface convective heat transfer, and pitot-pressure flow-field surveys were obtained.[47] A sketch of the model showing the basic model geometry and dimensions is given in fig. 15. The model has a delta planform with leading-edge sweepback of 75° and total axial length, L, of 0.9144 m (3 ft). The forebody is an elliptic cone with a major-to-minor axis ratio of 4, and the afterbody has elliptical cross sections with a sharp straight-line trailing edge. The juncture between the forebody and afterbody occurs at 2/3 of the body length. The model nose was sharp.

Examples of the data showing windward centerline surface-pressure and heating distributions are given in figs. 16 and 17. Also shown are predictions of the windward pressures and heating from the Ames UPS code (an upwind parabolized Navier-Stokes solver) with the Baldwin-Lomax turbulence model. There is generally good agreement between the windward pressure and heating data and the predictions, with greater differences at the higher angles of attack where the forebody pressures and heating are underpredicted .

Experimental pitot-pressure profiles of the shock layer for the afterbody centerline at x/L = 0.8 are compared with computations in fig. 18 for various angles of attack. The predictions are considered in good agreement overall with experiment except near the bow wave because of grid resolution. On the windward side, the merging of the viscous and expansion regions of the flow are also captured by the code.

7.3 Generic Single Expansion Ramp Nozzle Experiment

This experiment was conducted in the Ames 3.5' HWT at Mach 7.3 and a Reynolds number of 150 million/ft. A photograph of the model is shown in fig. 19. CFD was applied to design the model. Pressures, 5-hole pitot probe surveys, and ramp boundary layer profiles are available along with flow visualization. Navier-Stokes solutions are now being performed. An example of the results showing a comparison of the measured and computed shock system taken from ref. 67 is given in fig. 20. Very good agreement is observed.

8. CONCLUDING REMARKS

A comprehensive data base for CFD code validation was reviewed and experiments selected that provide a focused basis for evaluating code development. Two types of experiments were selected for each major flow component: building block experiments for simple flows that can verify physics and chemistry modeling and benchmark experiments that can validate forebody, inlet, combustor, and nozzle codes. Major gaps in the data base exist for the real gas conditions associated with flight, for reacting combustor flows, and for reacting nozzle flows.

In spite of these gaps, data to assess physical modeling for turbulent boundary layers, shock interactions with laminar and turbulent boundary layers, and combustor injector interactions are available. Similarly, some data on chemistry modeling for simple external aerodynamic flows and internal flows involving mixing of hydrogen and air were identified that can provide partial validation of the real gas aspects of the codes. Benchmark experimental data, mostly at enthalpy conditions below those associated with hypersonic flight, are also available for assessing predictions of various 3-D algorithms and their associated physical modeling assumptions.

While most of the recommended experiments provide the essential information for initiating computations, it would be prudent to establish unified input conditions, data presentation format, and error analysis for each of them. Precedents for such undertakings have already been established (see, e.g., refs. 68-70). A team of experts, knowledgeable in CFD and EFD, could undertake the steps necessary to see that this is accomplished in a timely fashion.

9. REFERENCES

1. Marvin, J. G., "Accuracy Requirements and Benchmark Experiments for CFD Validation," Symposium on Validation of Computational Fluid Dynamics, AGARD CP-437, 1988.

2. Marvin, J. G. and Holst, T. L., "CFD Validation for Aerodynamic Flows - Challenge for the '90's,". AIAA Paper 90-2995, AIAA 8th Applied Aerodynamics Conference, August 20 - 22, 1990/Portland, Oregon.

3. Raper, J. L, Carter, H. S., Hinson, W. F., and Morris, W. O., "Basic Measurements from a Turbulent-Heating Flight Experiment on a 5° Half-Angle Cone at Mach 20 (Reentry F)," NASA TMX-2308, 1971. See also NASA TMX-2584, 1972 and NASA TMX-2282, 1977.

4. Sanator, R. J., De Carlo, J. P., and Torillo, D. T., "Hypersonic Boundary-Layer Transition Data for a Cold-Wall Slender Cone," AIAA J., Vol. 3, No. 4, April 1965, pp. 758-80.

5. DiCristina, V., "Three-Dimensional Laminar Boundary-Layer Transition on a Sharp Cone at Mach 10," AIAA J., Vol. 8, No. 5, May 1970, pp. 852-856.

6. Chen, F. J., Malik, M. R., and Beckwith, I. E., "Boundary-Layer Transition on a Cone and Flat Plate at Mach 3.5," AIAA J., Vol. 27, No. 6, June 1989.

7. Stetson, K. and Rushton, "Shock Tunnel Investigation of Boundary Layer Transition at M=5.5," AIAA J., Vol. 5, No. 5, May 1967, pp. 899-905.

8. Owen, F. K. and Horstman, C. C., "On the Structure of Hypersonic Turbulent Boundary Layers," JFM , Vol. 53, part 4, pp. 611-636, 1974. See also AIAA J., Vol. 10, No. 6, pp. 769-775, June 1972.

9. (Flow Case 8101,2), "The 1980-81 AFOSR/HTTM-Stanford Conference on Complex Turbulent Flows," Vols. I, II and III, Ed. S. J. Kline et al., 1982.

10. Strawa, A. W., Molvik, G., Yates, L., and Cornelison, C., "Experimental and Computational Results for 5 Degree Blunt Cones with Shock Generators at High Velocity," AIAA Atmospheric Flight Mechanics Conference, Boston, MA, Aug. 1989, AIAA Paper 89-3377.

11. Spurk, J. H., "Experimental and Numerical Nonequilibrium Flow Studies", AIAA J., Vol. 8, pp. 1039-1045, 1970.

12. Hornung, H. G., "Non-equilibrium Dissociating Nitrogen Flow Over Spheres and Circular Cylinders," JFM, Vol. 53, pp. 149-176, 1772.

13. Lewis, J. E., Gran, R. L., and Kubota, T., "An Experiment on the Adiabatic Compressible Turbulent Boundary Layer in Adverse and Favorable Pressure-Gradients," J. Fluid Mechanics, Vol. 51, pt. 4, 1972, pp. 657-672.

14. Taylor, M. W., "A Supersonic Turbulent Boundary Layer on Concavely Curved Surfaces," Princeton, Gas Dyn. Lab. Rep. MAE 1684, 1984.

15. Fernando, E. M. and Smits, A. J., "A Data Compilation for a Supersonic Turbulent Boundary Layer Under Conditions of an Adverse Pressure Gradient," Princeton, Gas Dynamics Lab. Rep. MAE 1746.

16. Jayaram, M., Taylor, M. W., and Smits, A. J., "The Response of a Compressible Turbulent Boundary Layer to Short Regions of Concave Surface Curvature," J. Fluid Mech., 175, pp. 343-362.

17. Carver, D. B., "Heat Transfer, Surface Pressure and Flow Field Surveys on Conic and Biconic Models with Boundary Layer Trips at Mach 8 - Phases IV and VI," Calspan/AEDC Div., AEDC-T5R-80-V14, 1980.

18. Christophel, R. G., Rockwell, W. A., and Neumann, R. D., "Tabulated Mach 6 3-D Shock Wave-Turbulent Boundary Layer Interaction Heat Transfer Data (Supplement)," AFFDL-TM-74-212-FXG-Supplement, 1975 and Law, C. H., "Two-Dimensional Compression Corner and Planar Shock Wave Interactions," AFFDL-TR-65-36, 1966.

19. Coleman, G. T. and Stollery, J. L., "Heat Transfer from Hypersonic Turbulent Flow at a Wedge Compression Corner," J. Fluid Mechanics, Vol. 56, 1972, pp. 741-752.

20. Holden, M. S., Havener, A. G., and Lee, C. H., "Shock Wave/Turbulent Boundary Layer Interaction in High-Reynolds-Number Hypersonic Flows," CUBRC-86681, 1986 and Holden, M. S., "Experimental Studies of Quasi-Two-Dimensional and Three-Dimensional Viscous Interaction Regions Induced by Skewed-Shock and Swept-Shock Boundary Layer Interaction," AIAA Paper 84-1677, 1984.

21. Kussoy, M. I. and Horstman, C. C., "Documen-tation of Two- and Three-Dimensional Hypersonic Shock Wave/Turbulent Boundary Layer Interaction Flows," NASA TM-101075, 1989.

22. Kussoy, M. I. and Horstman, C. C., "An Experimental Documentation of a Hypersonic Shock-Wave Turbulent Boundary Layer Interaction Flow - With and Without Separation," NASA TM X-62412, 1975.

23. Fernholz, H. H., Finley, P. J., Dussauge, J. P., and Smits, A. J., "A Survey of Measurements and Measuring Techniques in Rapidly Distorted Compressible Turbulent Boundary Layers," AGARDograph 315, 1989. and Smits, A. J., and Muck, K. C., "Experimental Study of Three Dimensional Shock Wave/Turbulent Boundary Layer Interactions," J. Fluid Mechanics, Vol. 182, Sept. 1987, pp. 291-314.

24. Zheltovodov, A. A., Zaylichny, E. G., Trofimov, V. M., and Yakovlev, V. N., "Investigation of Heat Transfer and Turbulence in Supersonic Separation," ITPM Preprint 22-87, 1987.

25. Knight, D. D., Horstman, C. C., Bogdonoff, S. M., and Shapey, B. L., "The Flowfield Structure of the 3-D Shock Wave-Boundary Layer Interaction Generated by a 20 deg. Sharp Fin at Mach 3," AIAA Paper 86-0343, 1986.

26. Kim, K. S., Lee, Y., Alvi, F. S., Settles, G. S., and Horstman, C. C., "Laser Skin Friction Measurements and CFD Comparison of Weak-to-Strong Swept Shock/Boundary-Layer Interactions," AIAA Paper 90-0378, 1990.

27. Brown, J. L., Kussoy, M. I., and Coakley, T. J., "Turbulent Properties of Axisymmetric Shock-Wave/Boundary-Layer Interaction Flows," Turbulent Shear-Layer/Shock-Wave Interactions, edited by Delery, J., Springer-Verlag, Berlin, 1986, pp. 137-148 and Dunagan, S. E., Brown, J. L., and Miles, J. B., "Interferometric Data for a Shock-Wave/Boundary-Layer Interaction," NASA TM-88227, 1986.

28. Brown, J. D., Brown, J. L., and Kussoy, M. I., "A Documentation of Two- and Three-Dimensional Shock-Separated Turbulent Boundary Layers," NASA TM-101008, July 1988.

29. Settles, G. S., Horstman, C. C., and McKenzie, T. M., "Flowfield Scaling of a Swept Compression Corner Interaction-A Comparison of Experiment and Computation," AIAA Paper 84-0096, 1984.

30. Kussoy, M. I. and Horstman, K. C., "Documentation of Two- and Three-Dimensional Shock-Wave/Turbulent-Boundary Layer Interaction Flows at Mach 8.2," NASA TM-103838, May 1991.

31. Wieting, A. R. and Holden, M. S., "Experimental Study of Shock Wave Interference Heating in Supersonic Flows," AIAA Paper 87-1511, 1987.

32. Holden, M. S. and Moselle, J. R., "Theoretical and Experimental Studies of Shock Wave-Boundary Layer Interaction on Compression Surfaces in Hypersonic Flows," ARL 70-0002, Jan. 1970.

33. Kussoy, M. I. and Horstman, K. C., "Intersecting Shock-Wave/Turbulent Boundary-Layer Interactions at Mach 8.3," NASA TM 103909, Feb. 1992.

34. McDaniel, J., Fletcher, D., Hartfield, R., Jr., and Hollo, S., "Staged Transverse Injection into Mach 2 Flow Behind a Rearward-Facing Step: A 3-D Compressible Flow Test Case for Hypersonic Combustor Code Validation," AIAA Paper 91-5071, AIAA Third International Aerospace Planes Conference, 3-5 December 1991.

35. Jarrett, O., Cutler, A. D., Antliff, P. R., Chitsomboom, F., Dancey, C. L., and Wang, J. A., "Measurements of Temperature, Density, and Velocity in Supersonic Reacting Flow for CFD Code Validation," Proc. of the 25th JANNIF Combustion Meeting, Huntsville, AL, 1988.

36. Cheng, T. S., Wehrmeyer, J. A., Pitz, R. W., Jarrett, O., and Northam, G. B., "Finite Rate Chemistry Effects in a Mach 2 Reacting Flow," AIAA 91-2320, June 1991. See also AIAA Paper 91-0181, Jan. 1991 and NASA CR-189544, 1991.

37. Marek, B., "Reacting Mixing Layer," NASA CP 10003, Vol. 5, 1988.

38. Peschke, W. T., "Hydrogen Fueled Scramjet Study," 26 JANNAF Combustion Meeting, CPIA, Oct. 1989.

39. (Flow Case 8500), "The 1980-81 AFOSR/HTTM-Stanford Conference on Complex Turbulent Flows,"Vols. I, II and III, Ed. S. J. Kline, et al., 1982.

40. Barrows, M. C. and Kurkov, A. P., "Supersonic Combustion of Hydrogen in Vitiated Air Steam Using Stepped-Wall Injections," AIAA Paper 71-721, AIAA/SAE 7th propulsion Joint Specialist Conference, June 1-18, 1971.

41. Kemp, H. and Owen, F. K., "Experimental Study of Nozzle Wall Boundary Layers at Mach No. 20-47," NASA TND-6965, October 1972.

42. "Hypersonic Research Engine Project-Phase IIA, Nozzle Program 3rd Interim Technical Data Report, Data Item No. 5555-3.02," December 14-March 13, 1967, NASA Contract No. NAS1-6666, Air Research Manufacturing Division of the Garrett Corp., Rpt. Ap-67-3129, January 11, 1988.

43. Lewis, L. and Carlson, D., "Normal Shock Location in Underexpanded Gas and Gas Particle Jets," AIAA J., Vol. 2, No. 4, April 1964, pp. 776-777.

44. "Report of the Working Group on Aerodynamics for Afterbodies," AIAA Advisory Report #226, June 1986.

45. (Problem VIII.2), "NonEquilibrium Flow in a Shock Tube," Workshop on Hypersonic Flows for Reentry Problem,. Part II co-organized by INRIA - Sophia Antipolis and GAMNI-SMAI, April 15-19, 1991, Antibes, France.

46. "Generic Option #2 Experimental Database/CFD Code Validation," Vol. 4, Blended Wing Body Aerothermal Model and Test Program, prepared by McDonnell Douglas, Sept. 1988. (Information Subject to Export Control Laws).

47. Lockman, W., Lawrence, S., and Cleary, J., "Experimental and Computational Surface and Flow-Field Results for an All-Body Hypersonic Aircraft," AIAA Paper 90-3067.

48. Wier, L. J., Reddy, D. R., and Rupp, G. D., "Mach 5 Inlet CFD and Experimental Results," AIAA Paper 89-2355, 25th Joint Propulsion Conference, 1989; see also Reddy, D. R., Benson, T. J., and Wier, L. J., "Computation of 3-D Viscous Flow Computation of Mach 5 Inlet with Experimental Data," AIAA Paper 90-0600.

49. Anderson, W. E. and Wong, N. D., "Experimental Investigation of a Large-Scale, Two-Dimensional, Mixed-Compression Inlet System," NASA TMX-2016, May 1970.

50. Mueller, J. N., Trexler, C. A., and Sounders, S. W., "Wind Tunnel Tests on a 3-Dimensional Fixed-Geometry Scramjet Inlet at M=2.30 to 4.60," NASA TMX-73933, March 1977.

51. Yanta, W. J., Collier, A. S., Spring, W. C., III, Boyd, C. F., and McArthur, J. C., "Experimental Measurements of the Flow in a Scramjet Inlet at Mach 4," AIAA Paper 88-01988.

52. Torrence, M. G., "Experimental Investigation of a Mach 6 Fixed-Geometry Inlet Featuring Swept External-Internal Compression Flow Field," NASA TN D-7998, October 1975.

53. Trexler, C. A. and Scuders, S. W., "Design and Performance at a Local Mach Number of 6 of an Inlet for an Integrated Scramjet Concept," NASA TN D-7944, August 1975.

54. Gnos, A. V., Watson, E. C., Seebaugh, W. R., Sanator, R. J., and DeCarlo, J. P., "Investigation of Flow Fields Within Large-Scale Hypersonic Inlet Models," NASA TN D-7150, April 1973.

55. "Generic Option #2 Experimental Database/CFD Code Validation," Vol. 6, Inlet Models and Test Programs, prepared by McDonnell Douglas, Sept. 1988. (Information Subject to Export Control laws).

56. Orth, R. C., Erdos, J. T., et. al., "Data Report for Parametric Scramjet Combustor Experiments Conducted in the Calspan Shock Tunnel - 3rd Entry," Vol. I, GASL TR-309, General Applied Science Laboratories, 1989.

57. Mikkelsen, K., McDonald, T., and Brasket, R., "Model Tests of NASP Generic Option 2 Exhaust Nozzle Configuration," Fluidyne Report 1570, May 1989.

58. Spaid, F. and Keener, E., "Experimental Results for a Hypersonic Nozzle/Afterbody Flowfield," paper to be presented at 17th AIAA Ground Testing Conf., July 6-8, 1992, Nashville, TN.

59. Cubbage, J. and Kirkham, F., "Investigation of Engine Exhaust Airframe Interference on a Cruise Vehicle at M=6," NASA TND-6060, January 1971.

60. Marvin, J. G. and Coakley, T. J., "Turbulence Modeling for Hypersonic Flows," NASA TM-1201079, June 1989.

61. Prabhu, D. K., Tannehill, J. G., and Marvin, J. G., "A New PNS Code for Chemical Nonequilibrium Flows," AIAA J., Vol. 26, No. 27, July 1988.

62. Bhutta, B. A., Lewis, C. H., and Cantz, F. A., "A Fast Fully Iterative Parabolized Navier Stokes Solver for Chemically Reacting Reentry Flows," AIAA Paper 85-926, June 1989.

63. Settles, G. S. and Dodson, L. J., "Hypersonic Shock/Boundary-Layer Interaction Database," NASA CR-177577, April 1991.

64. Horstman, C. C., "Hypersonic Shock-Wave Turbulent-Boundary-Layer Interaction Flows - Experiment and Computation," AIAA Paper 91-1760, Honolulu, HI, Jun. 1991.

65. Knight, D. D., Hortsman, C. C., and Monson, D. J., "The Hypersonic Shock Wave-Turbulent Boundary Layer Interaction Generated by a Sharp Fin at Mach 8.2," AIAA Paper 92-0747, 30th Aerospace Sciences Meeting, 1992.

66. Tam, T. C., Brock, N. J., Cavolowsky, J. A., and Yates, L. A., "Holographic Interferometry at the NASA-AMES Hypervelocity Free-Flight Aerodynamic Facility," AIAA Paper 91-0568, Jan. 1991.

67. Ruffin, S. M., Venkatapathy, E., Lee, S. H., Keener, E. R., and Spaid, F. W., "Single Expansion Ramp Nozzle Simulations," AIAA Paper 92-0387, 30th Aerospace Sciences Meeting, Jan. 1992.

68. Fluid Dynamics Panel Working Group 04: "Experimental Data Base for Computer Program Assessment". AGARD-AR-138, 1979.

69. "The 1980-81 AFOSR/HTTM Stanford Conference on Complex Turbulent Flows," Vol. I, Editors, Kline, et. al., 1992.

70. Fluid Dynamics Panel Working Group 07: "Test Cases for Inviscid Flow Field Methods," AGARD-AR-211, 1985.

Table 1 Forebody building block data base.

Experiment(ref. no.)	3	4	5	6	7	8	9	10	11	12	13	14	15	16	17
Mach No.	20	10	10	3	5.5	7	0~6	15	9~9.5	6	4	3	3	3	8
Re No.x(E-06)		2/ft	2/ft	12	2~8	25	-	.5~1	.05~.06	.006~.01	5	63/m	63/m	63/m	3.7
2-d Geometry or Axisymmetric	✔	✔	✔	✔	✔	✔	✔	✔	✔	✔	✔	✔	✔	✔	✔
3-d Geometry															
Angle Of Attack(deg.)	0	0	0,4	0	0			0~20	0			0	0	0	0, 10
Physical And Chemical Modeling Req'mts															
Transition	✔	✔	✔	✔	✔										✔
Turbulence	✔					✔	✔				✔	✔	✔	✔	✔
Shock Boundary Layer Interactions*															
Entropy Layer Swallowing					✔			✔							✔
Equilibrium Chemistry	✔							✔							
Non equilibrium Chemistry								✔	✔	✔					
Wall catalysity									✔	✔					
Low Density Flow															
Adverse Press. Gradient											✔	✔	✔	✔	
Measurements															
Boundary Conditions	✔	✔	✔	✔	✔	✔	✔	✔	✔	✔	✔	✔	✔	✔	✔
Transition Location	✔	✔	✔	✔	✔	✔									
Wall Pressures	✔		✔			✔					✔	✔	✔	✔	✔
Heating Rates	✔	✔	✔	✔	✔	✔					✔				✔
Pitot Profiles						✔						✔	✔	✔	
Temperature Profiles						✔						✔	✔	✔	
Static Pressure Profiles						✔						✔	✔	✔	
Density Profiles						✔		✔		✔					
Velocity Profiles						✔					✔	✔	✔	✔	
Species Profiles															
Flow Visualization**								S		S					
Other(Specify)						cf,ch	cf,ch	Drag	standoff	standoff	cf	cf	cf	✔	
* See Inlet Unit Experiments															
** Shadowgraph															
Turbulece Measurements						✔								✔	

Table 2 Inlet building block data base.

Experiment(ref. no.)	18	19	20	21	22	23	24	25	26	27	28	29	30	31	32	33
Mach No.	6	9	11, 13	7	6.9	3	3	3	3	3	3	3	8.2	8	14	8.3
Re No.x(E-06)	10,30/ft	25	3.7/ft	5.8/m	35.8	.8~7.6	32/m	700/m	6/m	18/m	18/m	63/m	4.9/m		0.072	4.9/m
2-d Geometry or Axisymmetric		✔	✔	✔	✔	✔	✔						✔	✔	✔	
3-d Geometry	✔			✔				✔	✔		✔	✔	✔			✔
Physical And Chemical Modeling Req'mts																
Transition																
Turbulence	✔	✔	✔	✔	✔	✔	✔	✔	✔	✔	✔	✔	✔			✔
Shock Boundary Layer Interactions	✔	✔	✔	✔	✔	✔	✔	✔	✔	✔	✔	✔	✔	✔	✔	✔
Separation	✔	✔	✔	✔	✔	✔	✔	✔	✔	✔	✔	✔	✔	✔	✔	✔
Secondary/Corner Flows	✔														✔	
Mass Injection																
Bleed																
Equilibrium Chemistry																
Unsteady Flow																
Measurements																
Boundary Conditions	✔	✔	✔	✔	✔	✔	✔	✔	✔	✔	✔	✔	✔	✔	✔	✔
Transition Location				✔	✔											
Wall Pressures	✔	✔	✔	✔	✔	✔	✔	✔	✔	✔	✔	✔	✔	✔	✔	✔
Heating Rates	✔	✔	✔	✔	✔		✔						✔	✔	✔	✔
Pitot Profiles		✔	✔	✔	✔	✔	✔	✔	✔			✔	✔			✔
Temperature Profiles			✔	✔	✔	✔	✔						✔			✔
Static Pressure Profiles				✔	✔	✔	✔						✔			✔
Velocity Profiles				✔	✔	✔	✔			✔	✔					✔
Turbulence Quantities					✔	✔	✔			✔	✔					
Flow Visualization*	S			OF					OF	OF		OF	S,OF	S	S	OF
Other(Specify)					cf	cf		yaw	cf	rho (y)		yaw	yaw, cf		cf	yaw
* S=Shadograph, OF=Oil Flow, SP= Structure Plot																

Table 3 Combustor building block data base.

Experiment(ref. no.)	34	35	36	37	38	39	40
Mach No. for Experiment	2	2.1	2	<1	3	0~6	2.4
Flight MachNo. Simulated***	6c	6h	6c		7h	N/A	6h
2-d Geometry or Axisymmetric		✔	✔	✔	✔	✔	✔
3-d Geometry	✔						
Scale(in.) d=Duct Ht.; L=Flow Length	0.75d	0.75d	0.75d	4x8d	3d	N/A	2x3.5d
Physical And Chemical Modeling Req'mts							
Turbulence		✔	✔			✔	
Shock Interactions	ltd		✔		✔		
Shear Layers		✔	✔	✔	✔	✔	✔
Vortex/Shock Interaction							
Injector Interactions	✔	✔					
Finite Rate Chemistry		✔			✔		✔
Measurements							
Boundary Conditions	✔	✔			✔	✔	
Wall Pressures	✔			✔	✔		
Heating Rates					✔		
Skin Friction							
Pitot Profiles				✔			
Temperature Profiles		✔	✔	✔	✔		✔
Static Pressure Profiles	✔				✔		✔
Velocity Profiles	✔	✔	✔	✔			✔
Species Profiles	✔	✔		✔			✔
Turbulence Quantities	✔	✔	✔	✔	✔		✔
Flow Visualization*	LIF	✔	LIF	PLIF			
Other(Specify)						width	
* LIF= Laser Induced Fluorescence							
*** c=Cold Flow, Mc=1/3Mexp. ; h= Hot Flow, Flight Enthalpy Simulated							

Table 4 Nozzle building block data base.

Experiment(ref. no.)	41	42	43	44	45
Mach No. (Eqivalent Flight Or Test)	20~47	5~8		2.2	14
Mj		1~2.6	1.7~3	2	
Pj/Ptree stream			To 500	1.4	
2-d Geometry or Axisymmetric	✔	✔	✔	✔	✔
3-d Geometry					
Physical And Chemical Modeling Req'mts					
Turbulence	✔				
Shock Interactions			✔		
Shear Layers		✔		✔	
Secondary Flows					
Separation					
Relaminarization					
Finite Rate Chemistry		✔			✔
Measurements					none
Boundary Conditions		✔	✔	✔	✔
Transition/Relaminarization Location					
Thrust		✔			
Moments		✔			
Wall Pressures	✔	✔		✔	✔
Heating Rates					✔
Skin Friction					
Pitot Profiles	✔	✔			
Temperature Profiles	✔				✔
Static Pressure Profiles					✔
Velocity Profiles	✔				✔
Species Profiles					✔
Turbulence Quantities	✔				
Flow Visualization					
Other(Specify)		✔	Mach Disk	✔	

Table 5 Forebody benchmark data base.

Experiment(ref. no.)	17	46	47
Mach No.	8	11~20	7.4
Re No.x(E-06)	3.7	.3~32	5~25
2-d Geometry or Axisymmetric	✔		
3-d Geometry		✔	✔
Performance Requirements			
Lift		✔	
Drag		✔	
Heat Load		✔	
Inlet Profiles			
Flow Phenomena			
Transition	✔	✔	
Turbulence	✔	✔	
Shock Boundary Layer Interactions*			
Entropy Layer Swallowing	✔	✔	
Equilibrium Chemistry			
Non equilibrium Chemistry			
Wall Catalysity			
Low Density Flow			
Measurements			
Boundary Conditions	✔	✔	✔
Transition Location	✔	✔	
Lift		✔	
Drag		✔	
Wall Pressures	✔	✔	✔
Heating Rates	✔	✔	✔
Pitot Profiles		✔	✔
Temperature Profiles			
Static Pressure Profiles			
Velocity Profiles			
Species Profiles			
Flow Visualization**		S	S,OF
Other(Specify)			
* See Inlet Unit Experiments			
** S=Shadowgraph, OF=Oil Flow			

Table 6 Inlet benchmark data base.

Experiment(ref. no.)	48	49	50	51	52	53	54	55
Mach No.	3.5~4	3	2.3~4.6	4	6	6	7.4	11~16
Re No.x(E-06)/Ft	2.5	2.2	2.2	1.3	50.8	32.2	29.1	2~10.5
2-d Geometry	✔	✔		✔			✔	✔
3-d Geometry	✔	✔	✔		✔	✔		✔
Performance Requirements								
Mass Capture	✔	✔	✔			✔		
Kinetic Energy Efficiency						✔		
Pressure Recovery	✔	✔	✔		✔	✔	✔	
Heat Load								
Spillage Drag								
Exit Profiles	✔	✔	✔	✔		✔	✔	
Flow Phenomena								
Transition							✔	✔
Turbulence	✔	✔	✔	✔	✔	✔	✔	
Shock Boundary Layer Interactions	✔	✔	✔	✔	✔	✔	✔	✔
Separation	✔	✔	✔	✔				✔
Secondary/Corner Flows	✔	✔	✔	✔				✔
Mass Injection								
Bleed	✔	✔		✔	✔			
Equilibrium Chemistry								
Unsteady Flow	✔	✔		✔				✔
Measurements								
Boundary Conditions	✔	✔	✔	✔	✔	✔	✔	✔
Transition Location							✔	✔
Wall Pressures	✔	✔	✔	✔	✔	✔	✔	✔
Heating Rates								✔
Pitot Profiles	✔	✔	✔	✔	✔	✔	✔	✔
Temperature Profiles							✔	
Static Pressure Profiles	✔	✔	✔		•	•		
Velocity Profiles								
Flow Visualization*				S	S	Oil	S,OF	S
Other(Specify)				cf. <u'>				
* S=Shadowgraph/Schlerin, OF=Oil Flow								

Table 7 Nozzle benchmark data base.

Experiment(ref. no.)	56	57	58	59
Estimated Date Available	Now	Now	'92	Now
Mach No. (Flight Equiv. Or Free Stream	10	1~16	7.4	6
Mj	1.5~2	2&4.4	1.5~3.4	3.5
Pj/P free stream	6~60	20~200	6~100	1~4
2-d Geometry or Axisymmetric	✔	✔		
3-d Geometry			✔	✔
Performance Requirements				
Thrust		✔		
Moments		✔		
Heat Loads	✔	✔		
Flow Phenomena				
Turbulence				✔
Shock Interactions				
Shear Layers	✔		✔	
Secondary Flows	✔			✔
Separation				
Relaminarization				
Finite Rate Chemistry	✔		✔	✔
Multiple Jets				✔
Measurements				
Boundary Conditions-Inflow	Mass Fl.	Mass Fl.		
	Pitot	Pitot		
	Species			Gamma Jet
Transition/Relaminarization Location	✔			
Thrust		✔		✔
Moments				
Wall Pressures	✔	✔	✔	✔
Heating Rates or Wall Temperature	✔	✔	✔	
Skin Friction	✔		✔	
Pitot Profiles	✔	✔	✔	
Temperature Profiles				
Static Pressure Profiles	✔	✔	✔	
Velocity Profiles			✔	
Species Profiles	✔			
Flow Visualization	✔		✔	
Other(Specify)				

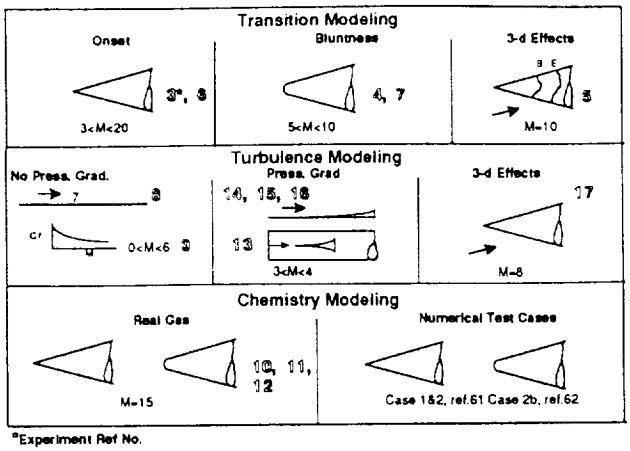

Fig. 1 Recommended forebody building block validation experiments.

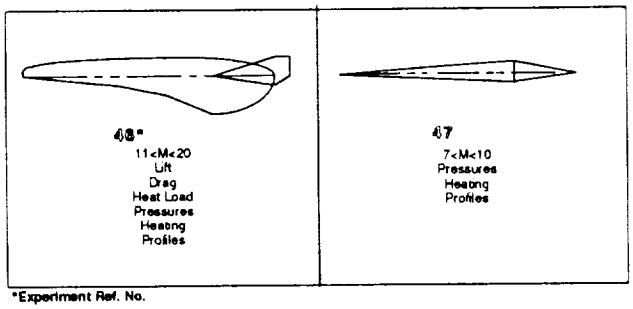

Fig. 2 Recommended forebody benchmark validation experiments.

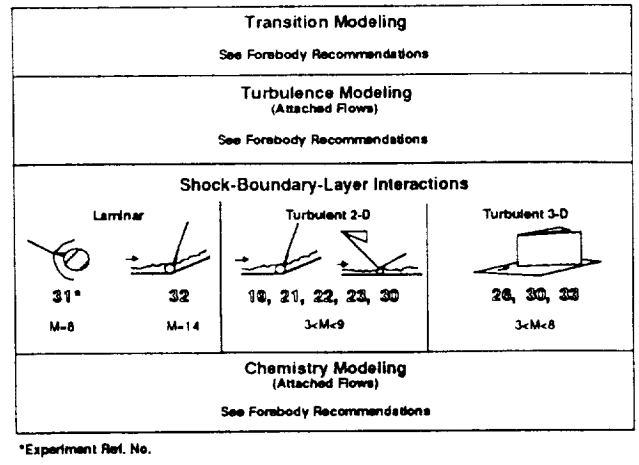

Fig. 3 Recommended inlet building block validation experiments.

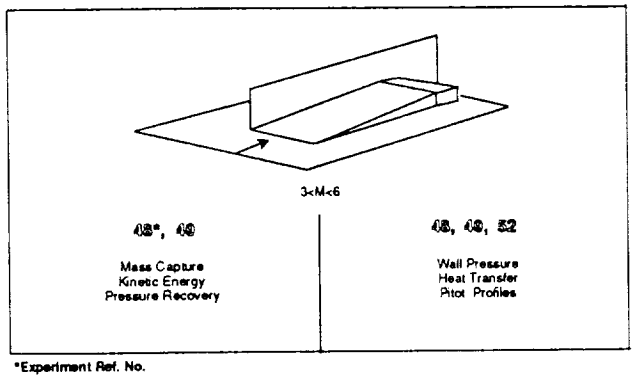

Fig. 4 Recommended inlet benchmark validation experiments.

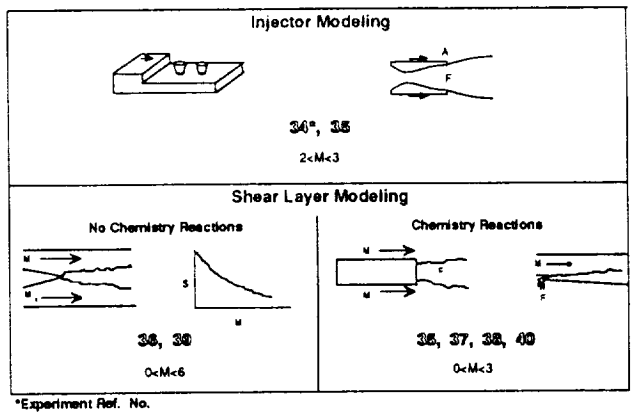

Fig. 5 Recommended combustor building block validation experiments.

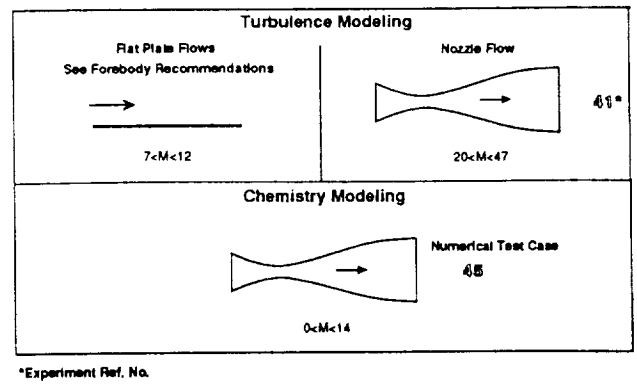

Fig. 6 Recommended nozzle building block validation experiments.

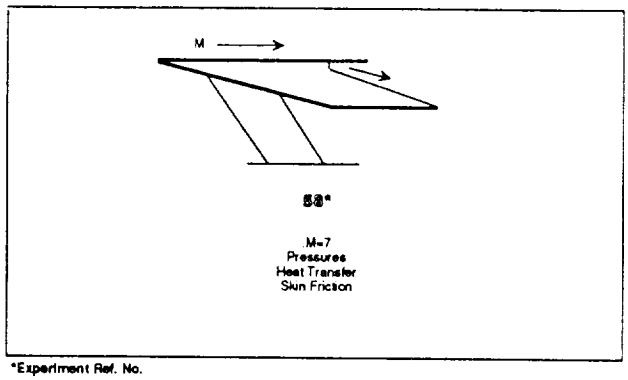

*Experiment Ref. No.

Fig. 7 Recommended nozzle benchmark validation experiments.

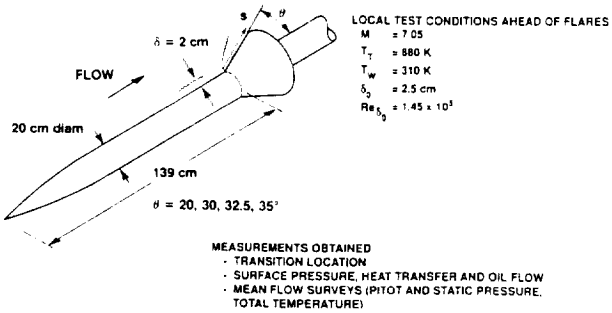

Fig. 8 Geometry and test conditions for an axisymmetric flare experiment.

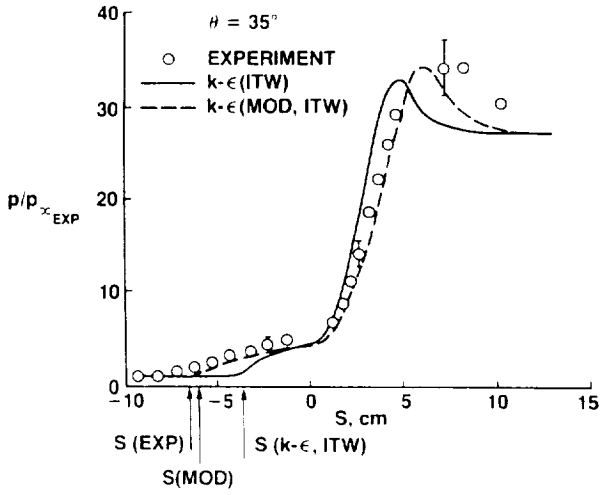

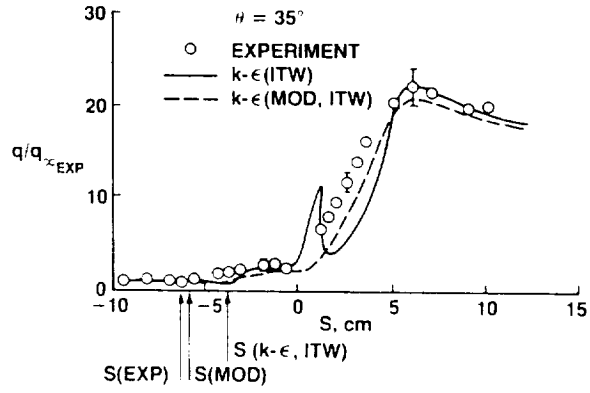

Fig. 9 Surface pressures and heating rates on an axisymmetric cylinder-flare.

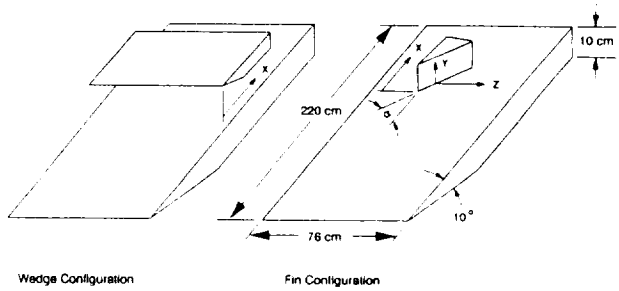

Fig. 10 Model geometries for impinging and swept shock interaction experiments.

$M_\infty = 8.2$, $Re_\infty/m = 5 \times 10^6$

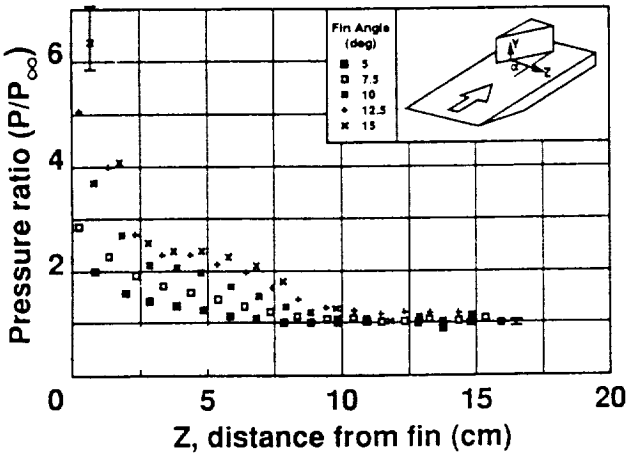

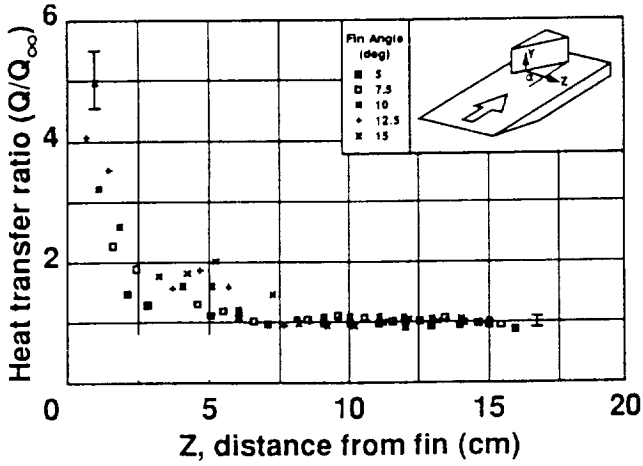

Fig. 11 Surface pressures and heating rates for a swept shock interaction.

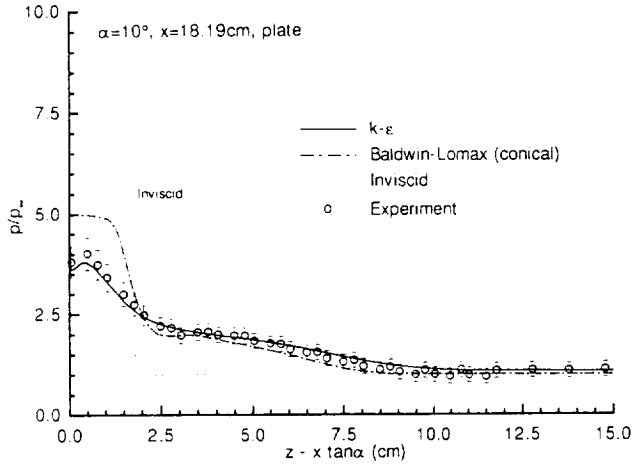

(a) Pressures

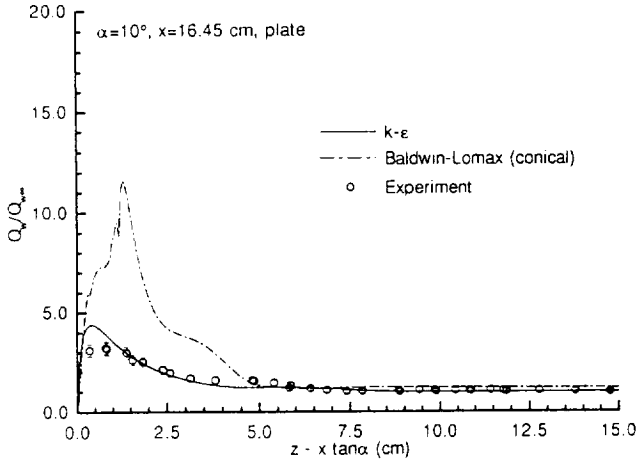

(b) Heat transfer

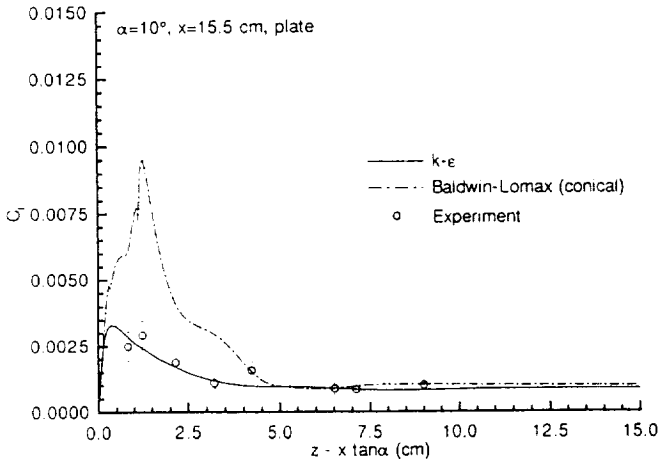

(c) Skin friction

Fig. 12 Comparisons of measurements and computations.

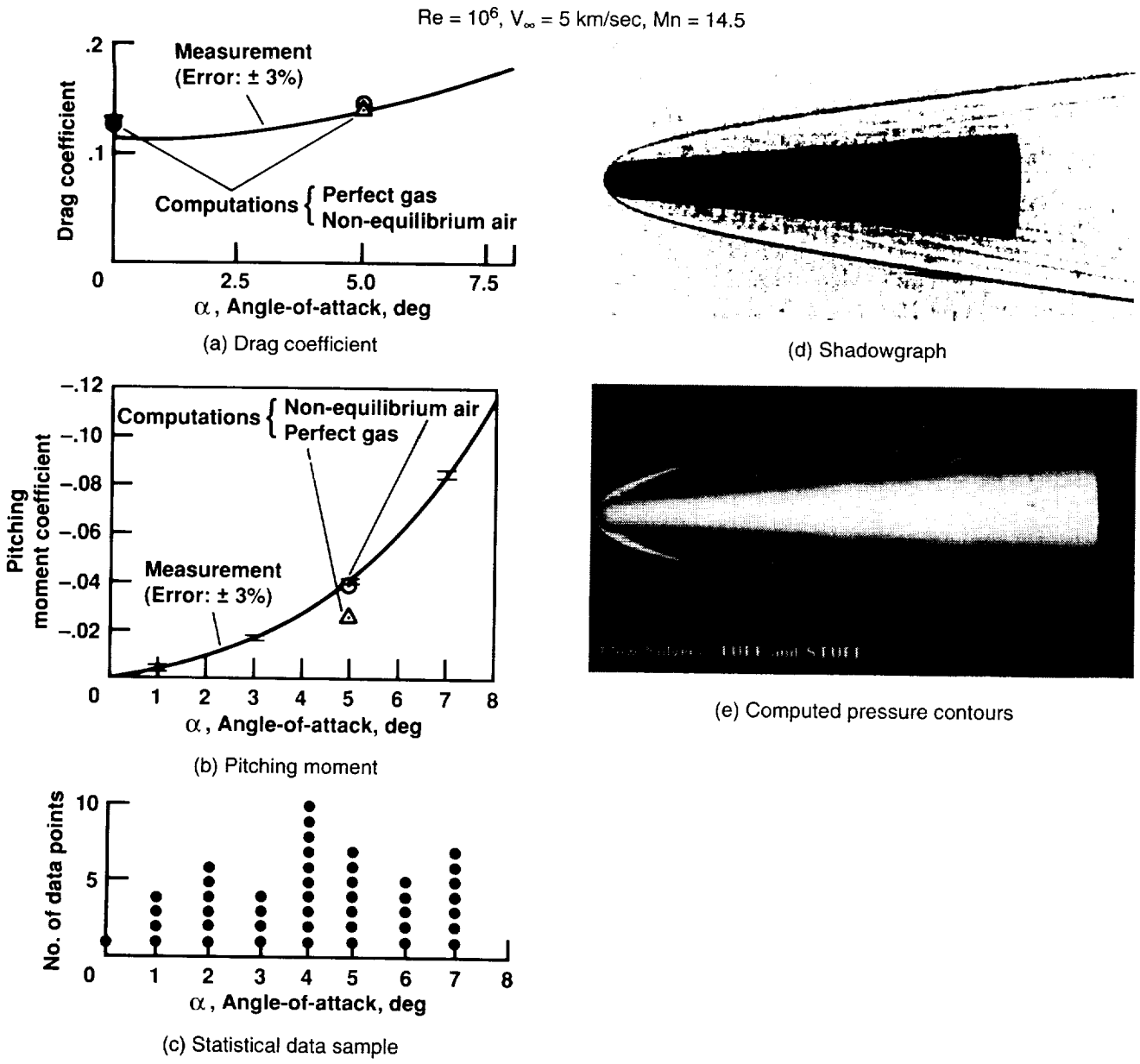

Fig. 13 Comparisons of force and moment coefficients and shadowgraph from a ballistic range experiment with computations.

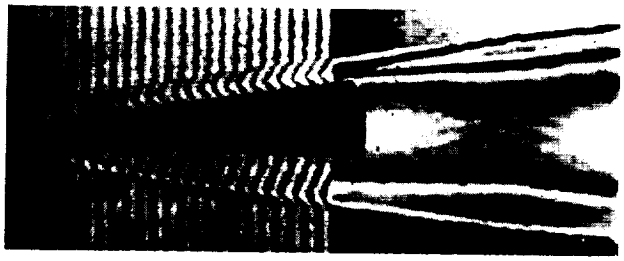

Fig. 14 Finite fringe interferogram and interpreted optical path from a ballistic range experiment.

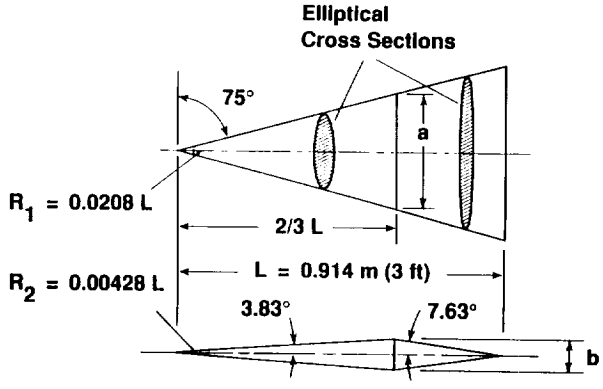

Forebody – Elliptic Cone (a/b = 4) with Sharp or Blunt Nose Tip
Afterbody – Elliptical Cross Sections with Sharp Trailing Edge

Fig. 15 Hypersonic All-Body model geometry and dimensions.

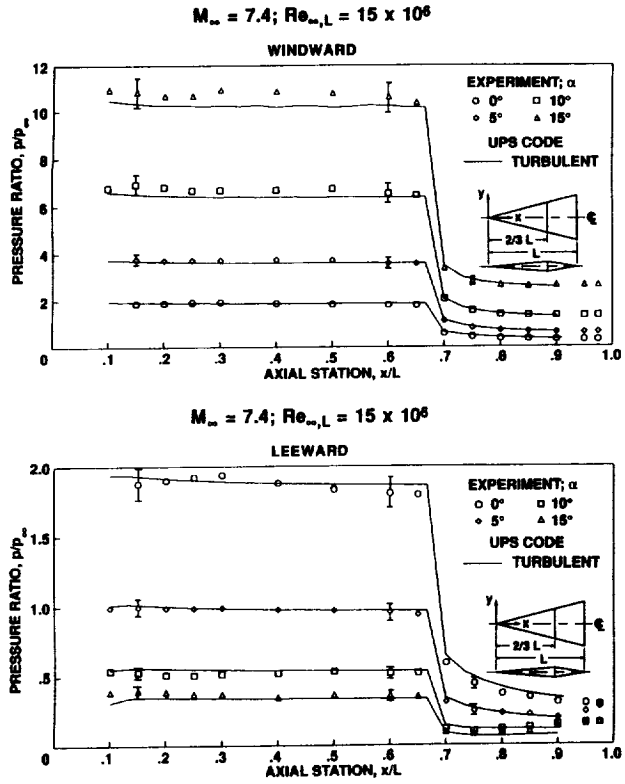

Fig. 16 Surface pressures on a hypersonic All-Body model.

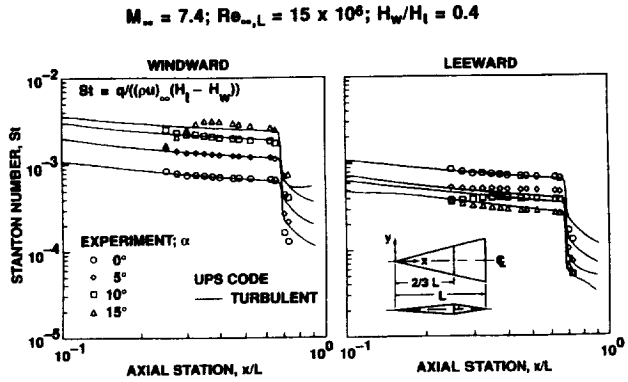

Fig. 17 Surface heat transfer on a hypersonic All-body model.

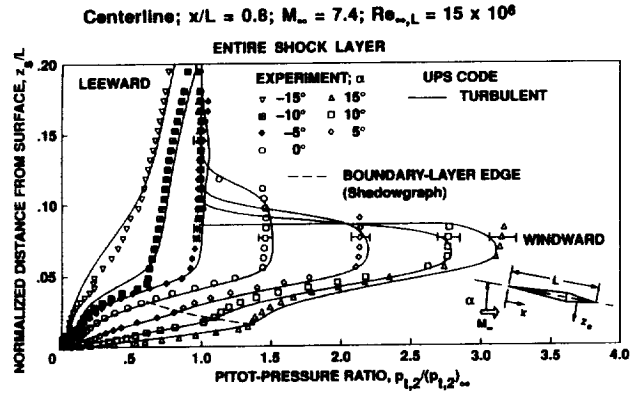

Fig. 18 Flow field pitot pressure profiles on a hypersonic All-Body model.

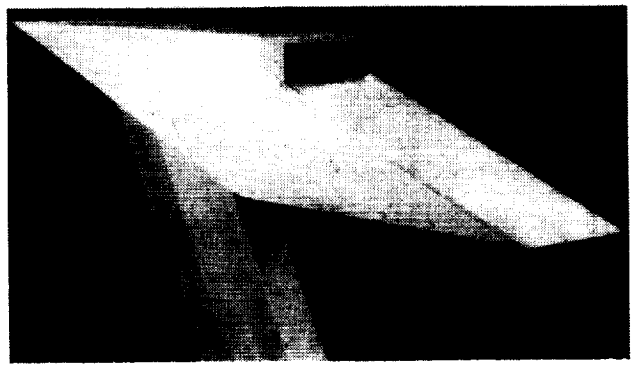

Fig. 19 Photograph of the SERN experiment.

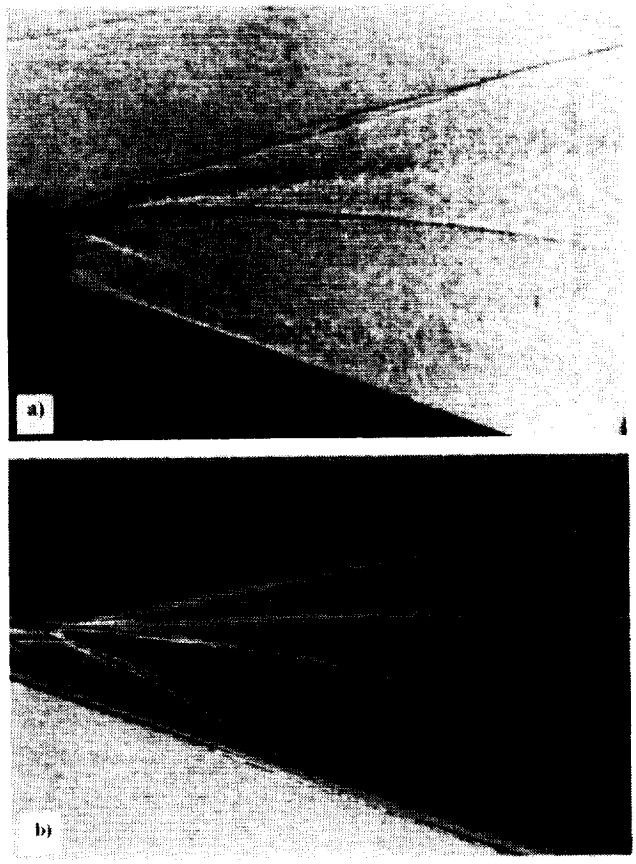

Fig. 20 Comparisons of nozzle shock patterns from experiment and a Navier-Stokes computation: (a) shadowgraph; (b) computation.

REPORT DOCUMENTATION PAGE

Form Approved
OMB No. 0704-0188

1. AGENCY USE ONLY *(Leave blank)*	2. REPORT DATE	3. REPORT TYPE AND DATES COVERED
	April 1992	Technical Memorandum

4. TITLE AND SUBTITLE

A CFD Validation Roadmap For Hypersonic Flows

5. FUNDING NUMBERS

505-59

6. AUTHOR(S)

Joseph G. Marvin

7. PERFORMING ORGANIZATION NAME(S) AND ADDRESS(ES)

Ames Research Center
Moffett Field, CA 94035-1000

8. PERFORMING ORGANIZATION REPORT NUMBER

A-92091

9. SPONSORING/MONITORING AGENCY NAME(S) AND ADDRESS(ES)

National Aeronautics and Space Administration
Washington, DC 20546-0001

10. SPONSORING/MONITORING AGENCY REPORT NUMBER

NASA TM-103935

11. SUPPLEMENTARY NOTES

Point of Contact: Joseph G. Marvin, Ames Research Center, MS 229-1, Moffett Field, CA 94035-1000 (415) 604-5390 or FTS 464-5390
This report was presented at the 70th Fluid Dynamics Panel Meeting and Symposium on Theoretical and Experimental Methods in Hypersonic Flows, Torino, Italy, May 4-8, 1992

12a. DISTRIBUTION/AVAILABILITY STATEMENT

Unclassified-Unlimited
Subject Category – 34

12b. DISTRIBUTION CODE

13. ABSTRACT ***(Maximum 200 words)***

A roadmap for CFD code validation is developed. The elements of the roadmap are consistent with air-breathing vehicle design requirements and related to the important flow path components: forebody, inlet, combustor, and nozzle. Building block and benchmark validation experiments are identified along with their test conditions and measurements. Based on an evaluation criteria, recommendations for an initial CFD validation data base are given and gaps identified where future experiments would provide the needed validation data.

14. SUBJECT TERMS

Computational fluid dynamics, Experimental fluid dynamics, Aeronautics, Fluid mechanics, Hypersonic flows

15. NUMBER OF PAGES

20

16. PRICE CODE

A02

17. SECURITY CLASSIFICATION OF REPORT	18. SECURITY CLASSIFICATION OF THIS PAGE	19. SECURITY CLASSIFICATION OF ABSTRACT	20. LIMITATION OF ABSTRACT
Unclassified	Unclassified		